Model to predict the response of correlation spectroscopy gas detection systems for CH_4

Paul Chambers, Ed A. Austin and John P. Dakin
Optoelectronics Research Centre, University of Southampton, Southampton, SO17 1BJ, UK.
Tel: +44-23-80593954, Fax: +44-23-80593149, E-mail: pac@orc.soton.ac.uk

***Abstract*—We present a comprehensive model of a correlation spectroscopy gas sensor for CH_4. Response and performance are predicted for typical fibre optic-coupled systems.**

***Index Terms*—CH_4, correlation spectroscopy, gas sensing**

I. Introduction

Absorption based correlation spectroscopy offers a method to selectively detect gases of industrial importance. We present a complete theoretical analysis of such a system for measurement of CH_4 gas.

Our model was used to predict system response to gases, signal-to-noise ratio (SNR) and cross-sensitivity performance, taking into account the effects of noise in measurements. The HITRAN database (http://www.hitran.com) was used to provide gas transmission spectra.

II. Principle of Operation

There are several methods for detecting gases using correlation spectroscopy [1-13]. An attractive absorption based method is the Complementary Source Modulation (CoSM) method [14-16]. This involves the alternate on/off switching of two broadband light sources in anti-phase, passing light from one of these sources through a reference cell containing the target gas (or gases) of interest for detection, and then combining this now partially-absorbed light beam with a fraction of unaffected light from the other source, in a proportion such as to give no net intensity modulation over an appropriately optically filtered bandwidth. The combined beam is then used to probe for the target gas. As the beam component which has passed through the reference gas sample now has less available optical energy lying within the narrow spectral regions of the target gas absorption lines, a net intensity modulation of the balanced combined beam will be re-established when it passes through a measurement cell containing the gas of interest. This induced intensity modulation is approximately proportional to the target gas concentration, as only differential absorption between the two beam components can contribute to a signal modulation. A typical schematic of an absorption based correlation spectroscopy gas sensing system, using fibre-optics, is shown in figure 1. The input signal detector is used to ensure balanced light power and the output signal detector is used to evaluate any intensity modulation resulting from test gas in the measurement cell.

III. System Model

It is important to model such a correlation spectroscopy system to predict performance, and to aid the very important choice of optical filter (or LED or super-luminescent optical fibre source). To do this, we have defined and analysed the parameters that determine the system performance.

We define the 'modulation depth', as the peak-to-peak AC signal variation arising at the output detector when gas is introduced into the measurement cell, divided by the mean DC level. The modulation depth is related to the transmission spectra of the reference cell, $T_{Ref}(\lambda)$, the measurement cell $T_{Meas}(\lambda)$, and the optical filter, $F(\lambda)$ by equation (1).

$$MD = 2\left(\frac{\int T_{Ref}(\lambda)T_{Meas}(\lambda)F(\lambda)d\lambda \int F(\lambda)d\lambda - \int T_{Ref}(\lambda)F(\lambda)d\lambda \int T_{Meas}(\lambda)F(\lambda)d\lambda}{\int T_{Ref}(\lambda)T_{Meas}(\lambda)F(\lambda)d\lambda \int F(\lambda)d\lambda + \int T_{Ref}(\lambda)F(\lambda)d\lambda \int T_{Meas}(\lambda)F(\lambda)d\lambda}\right) \quad (1)$$

If desired, the source spectra can be also, of course, taken into account in (1), by using additional spectral functions

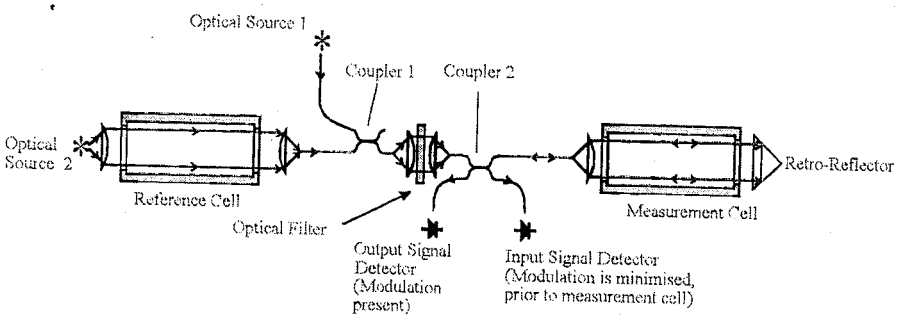

Figure 1 The CoSM correlation spectroscopy method for gas sensing.

as suitable product terms.

The modulation depth present when the measurement cell is filled with target gas is a measure of optical 'contrast'. To reduce sensitivity to environmental effects, such as dust in sensing cells or mechanical vibration, parameters should be chosen to maximize this parameter. However, for good selectivity, and to improve the SNR, it is also desirable to employ many gas absorption lines. These optima are discussed below, based on results from our model.

IV. Numerical results

In this section, after reproducing the transmission spectrum of CH_4 gas, we show results from our model. The modulation depth, SNR in measurements, and cross-sensitivity to a contaminant gas (water vapor) were modelled as a function of optical filter centre wavelength and bandwidth. We shall call this band-pass optical filter the 'selection filter', and assume it has a Gaussian shaped spectral response.

A. Transmission of CH_4 gas

Methane gas (CH_4) exhibits a strong rotational-vibrational 2v3 based absorption band at approximately 1.7μm, the spectrum of which is shown in Figure 2. Many commonly available optical sources and passive optical components function well at this wavelength so it is relatively straightforward to implement optical systems in this spectral region.

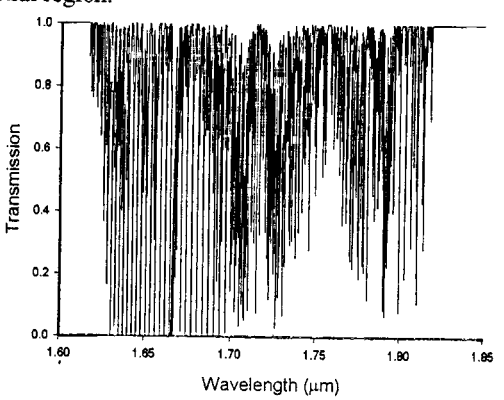

Figure 2 Transmission spectrum of CH_4 gas over a 1m path length at STP (transmission data obtained from HITRAN database).

B. Received modulation depth (optical 'contrast')

We calculated the effect on modulation depth of varying the central wavelength of the selection filter, assuming a narrow 2nm Full Width at Half Maximum (FWHM) bandwidth, see Figure 3.

Figure 3 shows a clear peak in modulation depth is achieved at an optical filter centre wavelength of 1666nm (co-incident with the Q-branch), where CH_4 has a closely-spaced set of absorption lines. The optimum bandwidth filter for accessing this peak was determined by plotting the modulation depth as a function of filter bandwidth, as shown in figure 4. This shows the peak in modulation depth actually occurs with a narrower filter bandwidth of 0.96nm. However, we will show that such a narrow filter is not a practical choice for good SNR (see Figure 8) and good selectivity (Figure 10). Poor stability can also result from choosing such a narrow bandwidth selection filter, despite high modulation depth, as the narrow linewidth can give high modal noise, arising from selective optical fibre mode coupling.

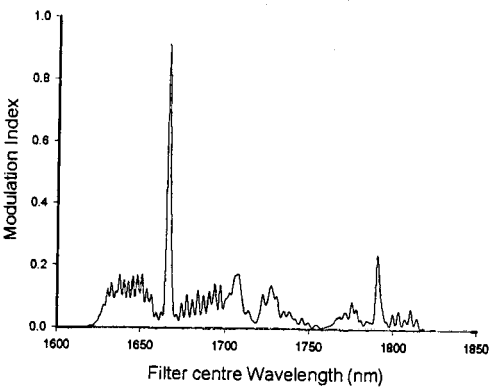

Figure 3 Modulation depth, as a function of selection filter centre wavelength, assuming reference and measurement cells contain 100% CH_4 at STP and a selection filter with 2nm FWHM bandwidth.

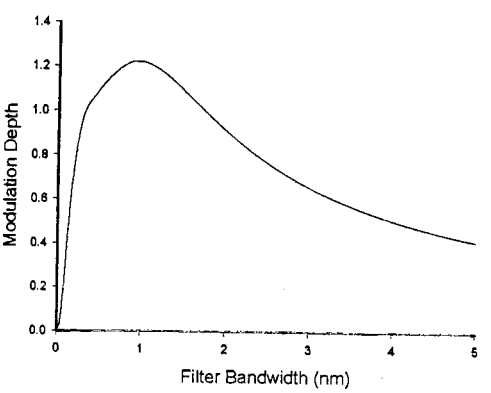

Figure 4 Modulation depth vs. filter bandwidth assuming reference and measurement cells, containing 100% CH_4, of length 1m at STP, and selection filter centre wavelength of 1666nm.

As this peak in modulation depth corresponds to, what we will show is a non-optimal narrow selection filter, we searched for other peaks requiring wider bandwidth filters. Figure 5 is a 3D plot, showing modulation depth as a function of optical selection filter width and central wavelength. Selection filters with centre wavelengths between 1.6μm and 1.85μm, and bandwidths between 1nm and 200nm were considered. As can be seen, the modulation depth response is highly complex, with several other narrow bandwidth maxima. These very narrow bandwidth (2nm) peaks are unsuitable, as previously discussed, and there are no further more suitable peaks. It

was therefore necessary to investigate the other system parameters, such as SNR.

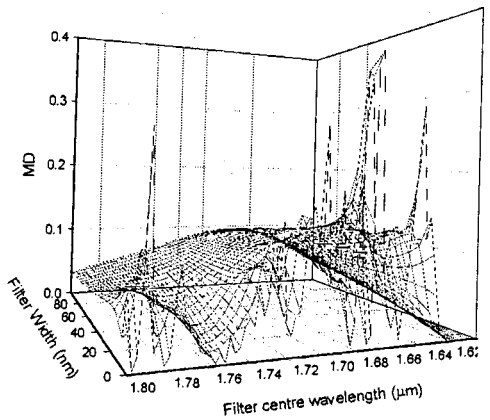

Figure 5 Modulation depth as a function of selection filter centre wavelength and bandwidth. The broad range of strong absorption lines make a very complex modulation depth response.

Before displaying results from our SNR calculations, the expected system response to CH_4 concentration (the 'calibration curve') is shown. Figure 6 plots the dependency of modulation depth on measurement gas cell concentration. This shows that, due to the strong absorption of the gas, there is a substantial non-linearity in the modulation index response at higher CH_4 gas concentrations. A selection filter bandwidth of 100nm was assumed for this calculation. As we shall see later, this is a realistic value.

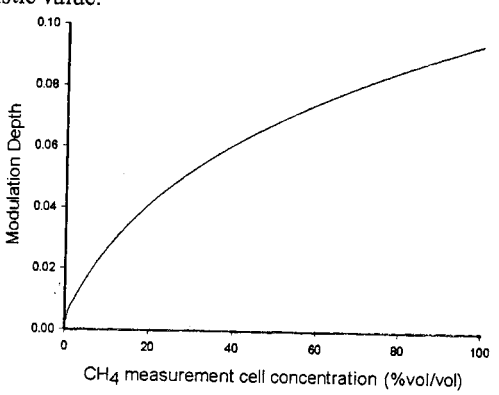

Figure 6 Modulation depth as a function of CH_4 concentration (%vol/vol) in the measurement cell. Reference and measurement cells are both of 1m length and the reference cell contains 100% CH_4 at STP. A selection filter having a bandwidth of 100nm at a centre wavelength of 1666nm was assumed.

C. Influence of selection filter on signal-to-nose ratio

Our model was used to predict system SNR performance, by predicting noise in measurements arising from fundamental photon statistics (2) (shot noise, which mostly dominates) and thermal noise in the optical receiver circuit (3). We assumed a spectral intensity at the output detector of 10nW/nm and a PIN optical detector, followed by a 10MΩ ($R_{Feedback}$) transimpedence amplifier.

$$I_{Photon\ noise} = \sqrt{2qI_{Sig}B} \quad (2)$$

$$V_{Thermal\ noise} = \sqrt{4kTBR_{Feedback}} \quad (3)$$

where q is electronic charge, k is the Boltzmann constant, T is absolute temperature (assumed to be 293°K), I_{sig} is the DC output current of the output detector and B is the detection bandwidth (assumed to be 0.1Hz).

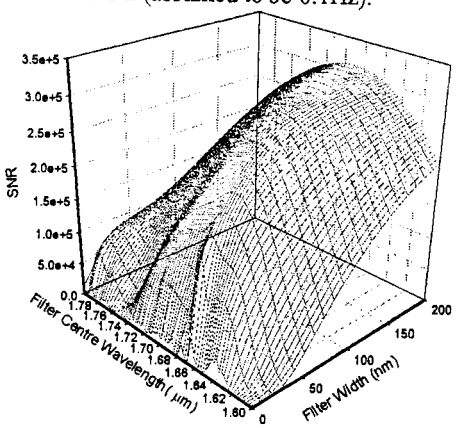

Figure 7 SNR in measurements as a function of selection filter choice.

Figure 7 plots the SNR expected as a function of selection filter bandwidth and centre wavelength, in the same range as the previous results. SNR shows little dependence on filter centre wavelength, especially near the optimum, where a wider bandwidth filter is used. Optimum SNR is attained with a filter bandwidth of approximately 197nm, i.e. much wider than the value required to maximize modulation depth (1.4nm).

Figure 8 plots SNR versus filter width, for a variety of received optical intensities. This shows that the absolute received light intensity has little effect on the optimal filter bandwidth for best signal-to-noise ratio. Note the very low SNR obtained with narrow filter widths.

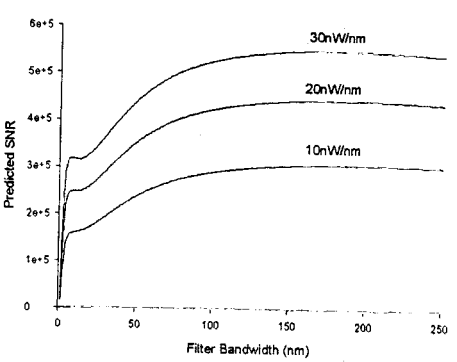

Figure 8 Predicted variation in SNR as the bandwidth of the Gaussian-shaped optical filter (centred at 1666 nm) is changed. This is shown for three detected output optical power levels. Reference and measurement gas cells are of 1m length and contain 100% CH_4 at STP.

D. Cross-sensitivity to water

Finally, we examined the cross sensitivity of the sensor to

contaminant gas. The correlation spectroscopy method, as described by equation 1, has the highly desirable property of having high selectivity, even when exposed to gas with non-coincident optical absorption lines in the same spectral region as that of the target gas. We illustrate this by modelling the response of the CH_4 sensor to water vapor, a likely contaminant species with some spectral absorption overlap. The transmission spectrum of water vapor is plotted in Figure 9.

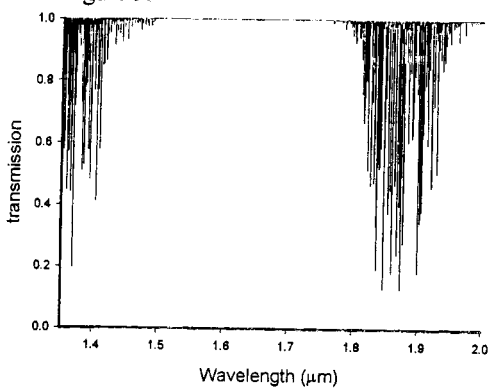

Figure 9 Transmission spectrum of water vapor over a 1m path length at STP. Transmission data obtained from HITRAN database, 0.05 bar partial pressure H_2O was assumed.

The cross-sensitivity of the CH_4 sensor to water vapor is shown in Figure 10, where the modulation depth expected with the measurement cell containing 0.05 bar (partial pressure) of water vapor is plotted as a function of selection filter bandwidth. Selection filters having the previously-determined optimum centre wavelength of 1666nm were assumed.

This shows the sensor starts to become more sensitive to water vapor when a filter bandwidth much in excess of 100nm is used. However the cross-sensitivity is always very small, 5% water vapor being equivalent to 21ppm CH_4 when a 100nm bandwidth filter is used, or 0.96% CH_4 when a 200nm bandwidth filter is used.

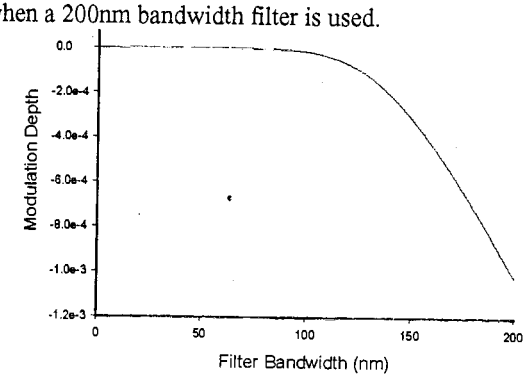

Figure 10 Modulation depth response to contaminant H_20. A selection filter centred at 1666nm, and the 1 m long reference and measurement cells contained 100% CH_4 and 5% (0.05 bar partial pressure) H_2O, respectively, at STP, were assumed.

V. Conclusions

We have used a theoretical model for gas detection systems using the CoSM scheme for absorption based correlation spectroscopy to predict the response and performance of a CH_4 sensor. Component characteristics for best signal-to-noise and selectivity to CH_4 were predicted.

This work has shown that, as expected, the response of such a system is strongly dependant of the type of optical selection filter chosen. For optimum modulation depth (measurement contrast), an optical filter having centre wavelength 1666nm and bandwidth 1.4nm would be chosen, but this would select so few lines that the other advantages of correlation spectroscopy [6,7,8,10] would be lost. To illustrate this, we have shown that, when other key aspects, such as achieving a good SNR, are taken into account it may be better to use an optical filter of somewhat higher bandwidth. The overall best SNR is achieved with a filter of width 197nm. Fortunately, following an initial peak, the modulation depth, or measurement contrast, does not drop very rapidly beyond widths of around 5nm so, choosing wider filter bandwidths to improve SNR should not lead to a significant reduction in modulation depth.

The sensor is expected to be highly selective. The presence of 0.05 bar water vapor would give an error of to 0.96% CH_4 if a 197nm bandwidth selection filter were used. If a 100nm bandwidth selection filter is chosen, this error falls to just 21ppm, because even fewer absorption lines coincide between the CH_4 reference gas and the water vapor contaminant gas.

VI. References

1. Hardwick, A. Berg, and D. Thingbo, *A fibre optic gas detection system*, Proc. 9th Int. Conf. on Optical Communications, 'ECOC 83' Geneva (1983), pp. 317.
2. T. Kobayashi, M. Hirana, and H. Inaba, *Remote monitoring of NO_2 molecules by differential absorption, using optical fibre link*, Appl. Opt., 20 (1981), pp. 3279.
3. K. Chan, H. Ito, and H. Inaba, *An optical fibre-based gas sensor for remote absorption measurements of low-level methane gas in the near-infrared region*, J. Lightwave Tech., LT-2 (1984), pp. 234.
4. S. Stueflotten *et al*, *An infrared fibre optic gas detection system*, Proc. OFS-94 int conf., Stuttgart, 1994, pp. 87.
5. R. Goody, *Cross-correlation spectrometer*, J. Opt. Soc. of Am., **58** (1968), pp. 900.
6. H. O. Edwards and J. P. Dakin, *A novel optical fibre gas sensor employing pressure-modulation spectroscopy*, Proc. OFS-90, int conf. , Sydney, Australia 1990, pp. 377, Dec 1990.
7. J.P. Dakin and H.O. Edwards, *Progress in fibre-remoted gas correlation spectroscopy*, Special issue of Optical Engineering, 31 (1992), pp 1616-1620
8. H. O. Edwards and J. P. Dakin, *Correlation spectroscopy gas sensing compatible with fibre-remoted operation*, Sens. actuators, B, Chem, 11 (1993), pp. 9.
9. J. P. Dakin, H. O. Edwards, and B. H. Weigl, *Progress with optical gas sensors using correlation spectroscopy*, Sens. actuators, B, Chem, 29 (1995), pp. 87.
10. J. P. Dakin (invited)., *Evolution of highly-selective gas sensing methods using correlation spectroscopy*, Advances in Optoelectronics for environmental monitoring, Erice, Sicily, Nov 1998.
11. J. P. Dakin, H. O. Edwards, and W. H. Weigl, *Latest developments in gas sensing using correlation spectroscopy*, Proc. SPIE Int. Conf., Munich, July 1995, paper 2508.
12. J. P. Dakin *Sensor for sensing the light absorption of a gas*, UK Patent Application GB2219656A.
13. H. O. Edwards and J. P. Dakin, *Measurements of cross-sensitivity to contaminant gases, using highly-selective, optical fibre-remoted methane sensor based on correlation spectroscopy*, Proc. SPIE Int. Conf "Chemical, biochemical & environmental fiber sensors"., Boston, Sept. 1991, SPIE Vol 1587 paper 33.
14. J. P. Dakin, M. J. Gunning, P. Chambers and E. A. Austin, *Fibre optic LFD-based correlation spectroscopy for O_2 detection, Proc* OFS-2002 int conf., 2002 Portland, Oregon 6-10 May 2002.
15. J. P. Dakin, M. J. Gunning and P. Chambers, *Detection of gases and gas mixtures by correlation spectroscopy*, Europt(R)ode VI, Manchester, 7-10 Apr 2002.
16. J.P.Dakin, M.J.Gunning, P.Chambers and Z.J.Xin, *Detection of gases by correlation spectroscopy*, Sensors & Actuators B: Chemical, accepted for publication.